J Neurophysiol 115: 1146–1156, 2016.
First published December 16, 2015; doi:10.1152/jn.00261.2015.

CALL FOR PAPERS | *Decision Making: Neural Mechanisms*

Modulation of impulsivity and reward sensitivity in intertemporal choice by striatal and midbrain dopamine synthesis in healthy adults

Christopher T. Smith,[1] Deanna L. Wallace,[2] Linh C. Dang,[2,3] Esther Aarts,[2,4] William J. Jagust,[2,3] Mark D'Esposito,[2] and Charlotte A. Boettiger[1,5]

[1]*Neurobiology Curriculum, University of North Carolina, Chapel Hill, North Carolina;* [2]*Helen Wills Neuroscience Institute, University of California, Berkeley, California;* [3]*Lawrence Berkeley National Laboratory, Berkeley, California;* [4]*Centre for Cognitive Neuroimaging, Donders Institute for Brain, Cognition and Behaviour, Radboud University Nijmegen, Nijmegen, The Netherlands; and* [5]*Department of Psychology & Neuroscience, Bowles Center for Alcohol Studies, and Biomedical Research Imaging Center, University of North Carolina, Chapel Hill, North Carolina*

Submitted 16 March 2015; accepted in final form 15 December 2015

Smith CT, Wallace DL, Dang LC, Aarts E, Jagust WJ, D'Esposito M, Boettiger CA. Modulation of impulsivity and reward sensitivity in intertemporal choice by striatal and midbrain dopamine synthesis in healthy adults. *J Neurophysiol* 115: 1146–1156, 2016. First published December 16, 2015; doi:10.1152/jn.00261.2015.— Converging evidence links individual differences in mesolimbic and mesocortical dopamine (DA) to variation in the tendency to choose immediate rewards ("*Now*") over larger, delayed rewards ("*Later*"), or "*Now* bias." However, to date, no study of healthy young adults has evaluated the relationship between *Now* bias and DA with positron emission tomography (PET). Sixteen healthy adults (ages 24–34 yr; 50% women) completed a delay-discounting task that quantified aspects of intertemporal reward choice, including *Now* bias and reward magnitude sensitivity. Participants also underwent PET scanning with 6-[^{18}F]fluoro-L-*m*-tyrosine (FMT), a radiotracer that measures DA synthesis capacity. Lower putamen FMT signal predicted elevated *Now* bias, a more rapidly declining discount rate with increasing delay time, and reduced willingness to accept low-interest-rate delayed rewards. In contrast, lower FMT signal in the midbrain predicted greater sensitivity to increasing magnitude of the *Later* reward. These data demonstrate that intertemporal reward choice in healthy humans varies with region-specific measures of DA processing, with regionally distinct associations with sensitivity to delay and to reward magnitude.

delay discounting; immediate reward bias; impulsive choice; putamen; ventral tegmental area

THE TENDENCY TO DISCOUNT delayed rewards, described variously as delay discounting (DD) or temporal discounting, is ubiquitous in the animal kingdom (Mazur 1987; Rachlin 2000). While some degree of DD is typical among healthy humans, a strong bias toward selecting immediate over larger delayed rewards, or "*Now* bias," is associated with multiple clinical conditions, including substance abuse (Becker and Murphy 1988; Reynolds 2006), attention deficit hyperactivity disorder (ADHD; Barkley et al. 2001; Paloyelis et al. 2010; Sonuga-Barke et al. 2008), and pathological gambling (Alessi and Petry 2003; Leeman and Potenza 2012). These clinical associations have helped to spark interest in understanding the neurobiology of such *Now* bias.

Data from humans and animals indicate that *Now* bias is highly heritable (Anokhin et al. 2011; Mitchell 2011). However, work in animals also indicates that *Now* bias can be pharmacologically modulated, particularly by dopamine (DA) (Dalley et al. 2008; Doya 2008; Winstanley 2011). Converging evidence also suggests the importance of frontal DA in regulating *Now* bias in humans. First, the Val^{158}Met polymorphism (rs4680) in the gene encoding the catechol-*O*-methyltransferase (COMT) enzyme, which regulates tonic frontal DA (Gogos et al. 1998; Kaenmaki et al. 2010; Karoum et al. 1994; Slifstein et al. 2008; Wu et al. 2012), predicts *Now* bias, with putatively lower tonic frontal DA being associated with greater *Now* bias among adults (Boettiger et al. 2007; Smith and Boettiger 2012). Moreover, COMT inhibition reduces *Now* bias (Kayser et al. 2012), and *COMT* genotype predicts the effects of acute changes in DA signaling on *Now* bias, according to a U-shaped model, with both low and high DA extremes predicting greater *Now* bias (Kelm and Boettiger 2013; Smith et al. 2014).

Striatal DA is also implicated in regulating *Now* bias by the clinical finding that patients with Parkinson's disease discount delayed rewards more heavily than age-matched control subjects do (Milenkova et al. 2011), particularly those with impulse control disorders (Housden et al. 2010), as well as by genetic studies (Eisenberg et al. 2007; Paloyelis et al. 2010) and by pharmacological manipulations that heavily modulate subcortical DA in humans (Acheson and de Wit 2008; de Wit 2009; de Wit et al. 2002; Hamidovic et al. 2008; Pine et al. 2010). Most of these pharmacology studies to date have produced inconsistent results, however, perhaps due to unaccounted for intrinsic variations in DA signaling (e.g., genetic or developmental) that could interact with pharmacological effects.

A recent positron emission tomography (PET) study of a sample of adult men with ADHD, some with comorbid cocaine dependence, found that DA transporter (DAT) occupancy by methylphenidate in the putamen, but not the caudate, significantly correlated with decreased *Now* bias on the drug

Address for reprint requests and other correspondence: C. A. Boettiger, Dept. of Psychology & Neuroscience, Davie Hall, CB #3270, Univ. of North Carolina, Chapel Hill, NC 27599-3270 (e-mail: cab@unc.edu).

(Crunelle et al. 2013). Two more recent reports from primarily clinical samples also support a role for lower subcortical DA being associated with increased *Now* bias (Ballard et al. 2015; Joutsa et al. 2015), although neither study included substantial numbers of healthy nonsmoking young adults. Notably, the degree to which COMT inhibition decreases synchrony between the putamen and the pregenual anterior cingulate cortex (pgACC) during *Now*/*Later* choices predicts how much COMT inhibition decreases *Now* bias (Kayser et al. 2012). COMT inhibition decreases *Now* bias more among more impulsive people, who in turn have lower DAT availability in the putamen (Costa et al. 2013) and both diminished midbrain D_2/D_3 autoreceptor binding and elevated amphetamine-induced striatal DA release (Buckholtz et al. 2010). The negative relationship between midbrain D_2/D_3 binding and trait impulsivity predicts that lower midbrain DA signaling may be associated with elevated *Now* bias, which also correlates with trait impulsivity (Mitchell et al. 2005).

Together, the data above support the idea that variations in subcortical DA also contribute to individual differences in *Now* bias, but no PET studies to date have investigated this question in a sample including only healthy young adult subjects. We hypothesized that those with relatively lower DA synthesis in the putamen would demonstrate elevated *Now* bias compared with those with higher putamen DA signaling. Although the supporting evidence is weaker, we also hypothesized that reduced midbrain DA synthesis would be associated with increased *Now* bias. Moreover, we predicted that such effects would be detected after controlling for effects predicted by *COMT* genotype. To test these ideas, we quantified subcortical DA synthesis in healthy young adults (ages 24–34 yr; 50% women), using PET with 6-[^{18}F]fluoro-L-*m*-tyrosine (FMT) uptake, a stable measure of DA synthesis capacity (DeJesus 2003). In a subsequent session, we measured *Now* bias with a validated DD task (Mitchell et al. 2005). We also determined *COMT* genotype for each participant and included *COMT* genotype as a covariate in our analyses.

MATERIALS AND METHODS

Sample characteristics. We invited 33 participants in a previous PET-FMT study at the University of California, Berkeley (UCB) to participate in this behavioral study; 16 participants accepted. Participants were neurologically and psychologically normal right-handed volunteers ages 24–34 yr (mean = 28, SD = 2.7; 50% women). Time between the FMT-PET scans and behavioral measurements was an average of 2.3 yr (SD = 1.1, range = 1.0–4.2 yr), similar to the elapsed time in previous studies measuring FMT uptake (Cools et al. 2009). Moreover, previous work has shown that binding potential (K_i) measures of presynaptic DA synthesis in the striatum are quite stable: within individual healthy subjects over a 7-yr span, the probability of K_i remaining within 18% of its original value is >95% (Vingerhoets et al. 1994). All participants gave written informed consent and were paid for participation, as approved by the UCB Committee for the Protection of Human Subjects.

COMT genotyping. We collected blood samples from participants, which were stored at the University of California, San Francisco (UCSF) DNA Bank and genotyped for the *COMT* Val^{158}Met polymorphism (rs4680) by the UCSF Genetics Core Facility (Lachman et al. 1996). *COMT* genotype was not available for one participant. *COMT* genotype distribution for the remaining 15 participants was 5 Met/Met, 6 Met/Val, and 4 Val/Val; this distribution did not differ from Hardy-Weinberg equilibrium ($\chi^2 = 0.58$, df = 1, $P = 0.447$).

Delay discounting task. Intertemporal choice behavior was assessed with a DD task described in detail previously (Fig. 1) (Altamirano et al. 2011; Kelm and Boettiger 2013; Smith et al. 2014). Subjects were given task instructions, completed a short practice, and then completed 8 blocks of 42 trials each. Subjects made a series of choices between smaller, sooner ("*Now*") and larger, later ("*Later*") hypothetical monetary rewards. Each trial began with an instruction cue, followed by two options. In each trial, the *Later* option was one of five amounts ($2, $5, $10, $20, or $100) available at one of five future delays (1 wk, 2 wk, 1 mo, 3 mo, or 6 mo), while the *Now* option amount was discounted from the *Later* amount by 5%, 10%, 15%, or 30%, and available "TODAY." The instruction cue indicated one of four trial types: WANT, DON'T WANT, SOONER, and LARGER (Fig. 1*A*); we consider the latter two conditions together as control (CON) trials. Reaction time (RT) is defined as the time between the point when the two options appeared and the time at which the participants indicated their choice. Accuracy in these CON trials verifies adherence to task instructions, and comparison of RT between the CON, WANT, and DON'T WANT conditions indicates whether additional cognitive processes are engaged in the WANT and DON'T WANT conditions, relative to the simple objective comparison in CON trials. Participants who fail to demonstrate sufficient accuracy in the CON condition trials or who fail to demonstrate longer RTs in the WANT relative to the CON condition are excluded. In this study, all participants met inclusion criteria for CON trial accuracy (mean: 96.9 ± 0.7%) and WANT-CON RT difference (mean: 475 ± 56 ms). Trial types were pseudorandomly ordered and weighted, with one-half WANT trials and one-sixth each of the other trial types. The WANT condition was most frequent because choice in that condition was our primary interest. Moreover, this weighting also promotes a prepotent tendency to select the preferred option, requiring inhibition in the DON'T WANT condition. Participants indicated their preferred option on WANT trials, their nonpreferred option on DON'T WANT trials, and the side with the sooner time or larger amount of money for SOONER and LARGER (CON) trials, respectively. The *Later* amount, delay time, percent discount, and left/right position (50/50) were pseudorandomly selected for each trial. We also collected the RT for each response. All subjects demonstrated the expected RT pattern across trial types (see above).

Behavioral data analyses. Our primary index of *Now* bias was the proportion of *Now* choices in the WANT condition, termed the impulsive choice ratio (ICR). We also examined ICR as a function of the delay time, estimated a logarithmic fit, and calculated the intercept and slope of the fit, which indicate impulsivity and sensitivity of discounting to increasing delay, respectively. We also determined the inferred ICR (iICR) from the DON'T WANT trials, as a function of delay time, calculating the average of the absolute difference between ICR and iICR at each delay. This value provides a measure of response control, with larger values indicating less controlled response selection (Mitchell et al. 2007). We also calculated the criterion interest rate acceptance threshold for each subject, which translates participant choices into an intuitive "real-world" approximation (Mitchell et al. 2007). To do so, we first calculated the simple interest rate for each trial according to the following equation:

$$\text{Interest Rate} = (\text{Amount}_{Later} - \text{Amount}_{Sooner})/(\text{Amount}_{Sooner} \times \text{Delay Time}) \quad (1)$$

We then plotted the percentage of trials in which the subject accepted the *Later* option against the interest rate and fitted the data with a logistic regression of the following form:

$$y = e^{(a+b\cdot X)}/\left[1 + e^{(a+b\cdot X)}\right] \quad (2)$$

Given the two-alternative forced-choice structure of our task design, we defined the interest rate criterion acceptance threshold (from the logistic fit) as the interest rate for which the subject chose the *Later* option 75% of the time. The criterion interest rate indicates the

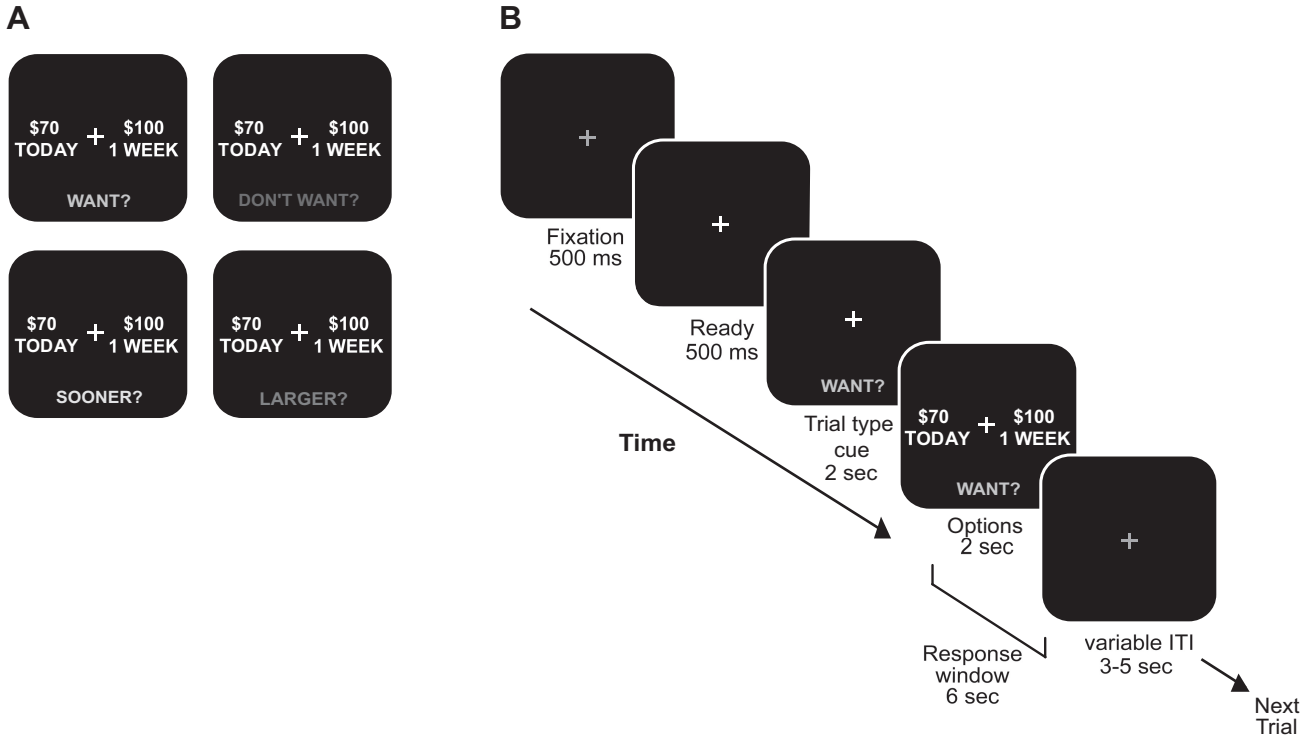

Fig. 1. Illustration of delay-discounting paradigm. *A*: depiction of the 4 trial types. The 4 trial types included WANT, DON'T WANT, and 2 objective choice types: SOONER and LARGER. The trial ratio was 1:2 WANT trials and 1:6 each for the other 3 trial types. *B*: the temporal sequence of trial events is shown for an example WANT trial. Illumination of a fixation cross ("Ready") marked each trial onset. An instruction cue informed the subject of the upcoming trial type. Two options were then presented while the Trial type cue remained on the screen. Options remained on the screen for 2 s, but subjects had 6 s to indicate their choice. Instruction cues for each trial type were depicted in a distinct color. ITI, intertrial interval.

simple interest rate at which the individual is three times more likely to accept the delayed reward than to opt for the immediate reward. For this measure, immediate reward bias would manifest as an unwillingness to wait for delayed rewards characterized by low to moderate interest rates.

In addition to ICR, a model-free choice metric, we also quantified the degree of impulsive choice, using the q-exponential discount function based on Tsallis statistics (Takahashi 2009; Takahashi et al. 2008):

$$\text{Discounted Value}(D) = 1/[1 + (1 - q)k_qD]^{1/(1-q)} \quad (3)$$

where D represents delay time and k_q and q are measures of impulsivity and of inconsistency in discount rate across delay times, respectively. To estimate k_q and q for each participant, we performed nonlinear curve fitting of each data set to *Eq. 3* with the Levenberg-Marquardt algorithm implemented in MATLAB (MathWorks, Natick, MA; Curve Fitting Toolbox, Custom Equation option). Discounted value was calculated as the cumulative selected-to-maximum dollar ratio at each delay D. In addition to estimating k_q and q, we also quantified the degree to which impatience declined as a function of delay time ("decreasing impatience," DI), as proposed by Prelac (2004) and implemented within the q-exponential discount function (Takahashi 2011):

$$\text{DI}_q(D) = k_q(1 - q)/[1 + k_q(1 - q)D] \quad (4)$$

with D, k_q, and q as defined in *Eq. 3*. DI quantifies the degree to which k_q changes with increasing delay time, with a rational (exponential) discount rate yielding a DI of zero and a positive DI indicating irrational intertemporal choice associated with immediate vs. delayed reward preference reversal with increasing delay time. We excluded $n = 3$ subjects from these analyses based on an inadequate fit by the q-exponential model (defined as an adjusted R^2 value < 0.2).

Statistical analysis. As ICR, k_q, q, and DI data in this sample were not normally distributed, we employed bootstrapping in unpaired t-tests comparing groups to eliminate concerns about violations of parametric assumptions. Repeated-measures ANOVAs were used to test for the effect of group on other DD task measures as well as on arc-sine root transformed ICR values. *COMT* genotype was included as a covariate in our analyses because of previous data showing *COMT* genotype effects on ICR (Boettiger et al. 2007; Paloyelis et al. 2010; Smith and Boettiger 2012). As the male-to-female ratio differed significantly between the High (2:6) and Low (6:1) midbrain FMT groups ($\chi^2 = 5.53$, $P = 0.019$), we also covaried for sex in our midbrain FMT analyses. Note that all reported means thus reflect the covariate adjusted (i.e., estimated marginal) means. Pearson's r or Spearman's ρ with bootstrapping was used for correlation analyses, as indicated, and 95% confidence intervals (CIs) are reported. Where sphericity was violated, we applied the Greenhouse-Geisser correction.

PET data acquisition. PET imaging and FMT synthesis were performed at Lawrence Berkeley National Laboratory; FMT was synthesized as described previously (VanBrocklin et al. 2004). FMT is metabolized by aromatic L-amino acid decarboxylase (AADC), a DA-synthesizing enzyme, the activity of which indexes the ability of dopaminergic neurons to synthesize DA given optimal substrate (DeJesus 2003). FMT is subsequently oxidized to 6-[^{18}F]fluorohydroxyphenylacetic acid, which is detected in PET-FMT scans. Signal intensity on PET-FMT scans thus indicates local DA synthesis capacity (Jordan et al. 1997).

PET scans were acquired with a Siemens ECAT-HR PET camera, as previously described (Landau et al. 2009). Each participant received a bolus injection of ~2.5 mCi of FMT into an antecubital vein. A dynamic acquisition sequence was acquired in 3D mode for a total of 89 min. We reconstructed FMT images with an ordered-subset expectation-maximization algorithm with weighted attenuation, fol-

lowed by scatter correction, and smoothing with a 4-mm full-width half-maximum (FWHM) kernel.

Structural MRI. We acquired two volumetric high-resolution magnetization-prepared rapid acquisition with gradient echo (MPRAGE) T1-weighted anatomical images from each participant on a 1.5-T Siemens Magnetom Avanto MRI scanner (Erlangen, Germany) with a 12-channel head coil (echo time = 3.58 ms; repetition time = 2,120 ms; voxel size = 1.0 mm^3, 160 axial slices; field of view = 256 mm; scanning time ≈ 9 min). The two images were averaged to obtain one high-resolution structural image, which was used to generate individual striatal and midbrain regions of interest (ROIs).

Regions of interest. We drew ROIs based on visual inspection of each subject's mean MPRAGE with FSLview. The dorsal putamen (Fig. 2*A*), dorsal caudate, and ventral striatum ROIs were drawn according to previously published guidelines (Mawlawi et al. 2001), based on the Mai atlas (Mai et al. 1997). The midbrain ROIs included both ventral tegmental area (VTA) and substantia nigra and were drawn on five consecutive axial slices, with the most caudal slice being the one in which the frontopontine fibers separated into left and right bundles and the substantia nigra was outlined clearly (Fig. 2*B*). Intrarater reliability and interrater reliability were both >95%. Following previously published methods, the reference region for calculating PET-FMT values was cerebellar gray matter (Braskie et al. 2008; Cools et al. 2009; Landau et al. 2009). Given the cerebellum's location posterior and adjacent to the midbrain, and the limited spatial resolution and blurring of PET signal, to avoid contaminating the cerebellar ROI with midbrain FMT signal only the posterior three-fourths of the cerebellum was included in the ROI.

PET data analysis. We reconstructed the FMT images with an ordered-subset expectation-maximization algorithm weighted by attenuation, corrected for scatter, and smoothed with a 4-mm FWHM kernel. We realigned the FMT images to the middle (12th) frame, to correct for movement during scanning using SPM8 (Ashburner et al. 2008; http://www.fil.ion.ucl.ac.uk/spm/). We coregistered the mean MPRAGE (and ROIs) to the mean image of all realigned frames in the FMT scan with FSL-FLIRT (version 4.1.2; http://www.fmrib.ox.ac.uk/fsl/). After coregistration, the ROI masks were thresholded at 0.5, ensuring high tissue probability. To create K_i images representing the amount of tracer accumulated in the ROIs relative to the cerebellar reference region, we used an in-house graphical analysis program implementing Patlak plotting (Logan 2000; Patlak and Blasberg 1985). We extracted average K_i values from the ROIs and computed associations between regional FMT uptake (K_i values) and the behavioral task measures described in RESULTS.

RESULTS

Low FMT K_i in the putamen predicts elevated Now bias. We predicted greater *Now* bias in those with relatively lower FMT K_i in the putamen, which we first quantified as the ICR (see MATERIALS AND METHODS). Indeed, in comparing the participants with bilateral putamen FMT K_i values below the group median (Low putamen FMT; see Fig. 2*A*, *center*, for example) to those above the group median (High putamen FMT; see Fig. 2*A*, *right*, for example), we observed significantly higher ICRs in the Low putamen FMT group (median = 0.80) relative to the High putamen FMT group (median = 0.50) in a bootstrapped ANOVA [$F_{(1,12)} = 5.27$, $P = 0.041$, $\eta^2 = 0.27$; Fig. 3*A*]. Notably, we also observed a negative correlation between putamen FMT K_i values and ICR (after partialing out *COMT* genotype effects): $r = -0.513$ (95% CI: −0.169, −0.807), $P = 0.060$. We next examined ICR as a function of the delay time (Fig. 3*B*). A mixed-effects 2 × 5 ANOVA found significant main effects of both group [$F_{(1,12)} = 6.28$, $P = 0.028$] and delay time [$F_{(4,48)} = 4.90$, $P = 0.002$] but no significant putamen FMT × delay interaction [$F_{(4,48)} = 0.38$, $P = 0.821$]. Direct comparison of the slope and intercept terms of the logarithmic fit to each subject's ICR as a function of delayed reward delay time found significant effects of putamen FMT on the intercept [$F_{(1,12)} = 8.38$, $P = 0.013$] but not the slope [$F_{(1,12)} = 0.49$, $P = 0.50$]. The intercept differences indicate more impulsive choice in the Low putamen FMT group, while the lack of difference between slopes indicates that the sensitivity of discounting to increasing delay is similar between groups (Mitchell et al. 2005). *Now* bias also varied as a function of the delayed reward amount (Fig. 3*C*). A 2 × 5 mixed-effects ANOVA found significant main effects of both

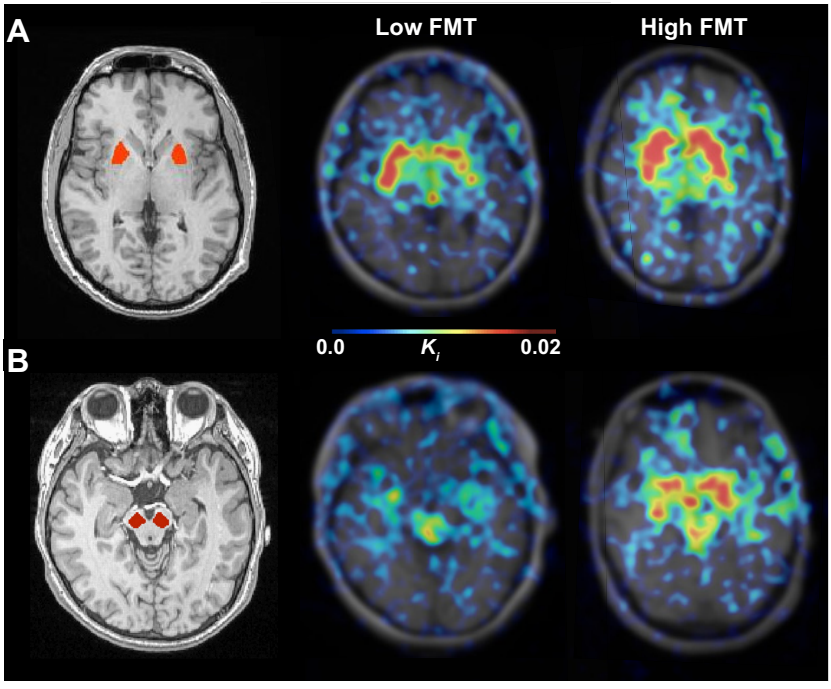

Fig. 2. Definition of regions of interest (ROIs). *A*: putamen ROIs. *Left*: the manually defined bilateral dorsal putamen ROIs superimposed on a high-resolution structural image for 1 participant in the study. Each participant's structural image was subsequently coregistered to a positron emission tomography (PET) image depicting 6-[^{18}F]fluoro-L-*m*-tyrosine (FMT) uptake, and binding potential (K_i) values (relative to the cerebellum) were extracted from the ROIs. *Center*: FMT uptake in a PET image at the level of the dorsal putamen in a Low putamen FMT subject. *Right*: putamen FMT uptake in a High putamen FMT subject. Both PET images are shown overlaid on the individual structural images. *B*: midbrain ROI. *Left*: the manually defined bilateral midbrain ROI superimposed on a high-resolution structural image of 1 study participant. *Center* and *right*: FMT uptake in example PET images overlaid on the individual structural image, from which binding potential values (relative to the cerebellum) were extracted within the ROI: low midbrain FMT subject (*center*) and High midbrain FMT subject (*right*).

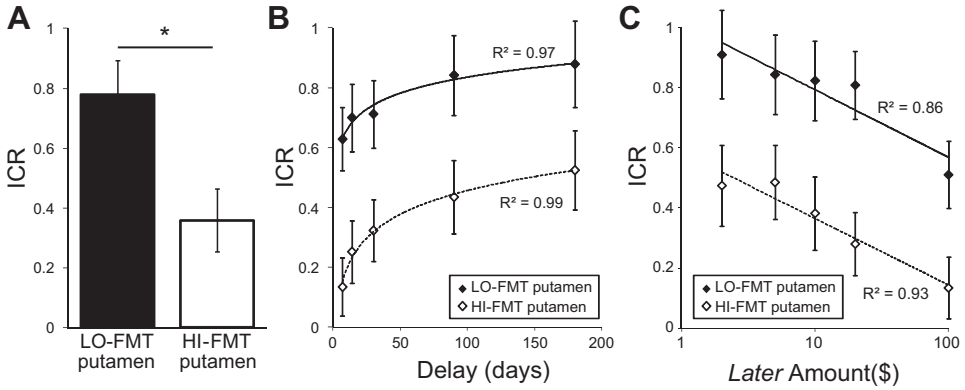

Fig. 3. *Now* bias is elevated in those with lower putamen FMT. *A*: covariate-adjusted impulsive choice ratio (ICR) in participants with below-median FMT signal in bilateral putamen (LO-FMT putamen) or above-median FMT signal in bilateral putamen (HI-FMT putamen). ICR differed significantly between groups [$F_{(1,12)} = 5.27$, $^*P = 0.041$]. *B*: covariate-adjusted ICR as a function of delayed reward time in the Low putamen FMT group and High putamen FMT group. *C*: covariate-adjusted ICR as a function of delayed reward amount in the Low putamen FMT group and High putamen FMT group. Values reflect estimated marginal means ± SE. Lines represent logarithmic fit of the group averaged data, with regression terms shown for each group.

putamen FMT [$F_{(1,12)} = 6.39$, $P = 0.026$] and *Later* amount [$F_{(4,48)} = 3.25$, $P = 0.019$] but no significant putamen FMT × amount interaction [$F_{(4,48)} = 0.41$, $P = 0.80$]. Direct comparison of the slope and intercept terms of the logarithmic fit to each subject's ICR by reward magnitude data found no significant group difference in either the average slope [Low putamen FMT: mean = −0.27 ± 0.17; High putamen FMT: mean = −0.22 ± 0.20; $t_{(14)} = -0.55$, $P = 0.59$] or intercept [Low putamen FMT: mean = 0.95 ± 0.38; High putamen FMT: mean = 0.66 ± 0.34; $t_{(14)} = 1.58$, $P = 0.136$]. Finally, we tested whether putamen FMT K_i values impacted subjects' criterion interest rate acceptance threshold (Mitchell et al. 2007), a metric that strongly covaries with ICR [Spearman's $\rho = 0.776$ (95% CI: 0.339, 0.989), $P < 0.001$] but more intuitively translates to "real-life" decision making. We found a significant and very large main effect of putamen FMT on the interest rate criterion threshold [Fig. 4; $F_{(1,12)} = 12.44$, $P = 0.004$, $\eta^2 = 0.481$], with the High putamen FMT group being willing to accept delayed rewards at significantly lower interest rates (Low putamen FMT: 21.13 ± 9.2%, High putamen FMT: 2.60 ± 9.08%). We also observed a negative correlation between putamen FMT K_i values and criterion interest rate (after partialing out *COMT* genotype effects): $r = -0.592$ (95% CI: −0.355, −0.822), $P = 0.026$.

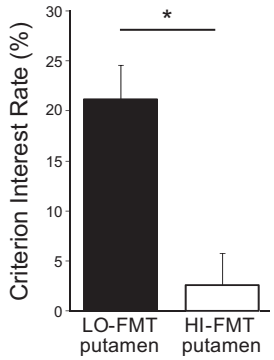

Fig. 4. Lower putamen FMT signal is associated with substantially elevated criterion interest rate threshold: covariate-adjusted criterion interest rate acceptance threshold in participants with below-median FMT signal in bilateral putamen (LO-FMT putamen) and above-median FMT signal in bilateral putamen (HI-FMT putamen). The criterion interest rate significantly differed between groups [$F_{(1,12)} = 12.44$, $^*P = 0.004$]. Conventions as for Fig. 3.

This *Now*/*Later* task includes objective choice CON trials; accuracy in these trials did not differ significantly between the Low putamen FMT and High putamen FMT groups [$F_{(1,12)} = 1.28$, $P = 0.28$]. The task also includes a control condition (DON'T WANT) in which participants are instructed to select the monetary reward option that they do not prefer. Comparing ICR in the WANT trials to iICR in the DON'T WANT trials provides a measure of response consistency. We did not detect a significant effect of putamen FMT on this measure of response consistency [see MATERIALS AND METHODS; $F_{(1,12)} = 0.06$, $P = 0.81$]. These results indicate that a difference in response consistency cannot explain the elevated *Now* bias observed in the Low putamen FMT group. We also observed no putamen FMT group effects on RT in the objective choice (CON) trials [$F_{(1,12)} = 3.21$, $P = 0.10$], subjective choice (WANT) [$F_{(1,12)} = 0.71$, $P = 0.42$], or DON'T WANT [$F_{(1,12)} = 0.41$, $P = 0.53$] trials.

As a measure of *Now* bias, ICR has several advantages. The first is its strong internal reliability, as indicated by the Cronbach's α for ICR in the present data set, which ranged between 0.96 and 0.98 across participants. The second is that ICR is an assumption-free metric, making it more robust than model-based metrics. In contrast, discounting rates (k) derived via curve-fitting using discounting models depend strongly on both the particular model's assumptions and the variability of the underlying data to be fit. Despite these caveats, recent studies have demonstrated the utility of the q-exponential discount function in parameterizing both *Now* bias (impulsivity; k_q) and the inconsistency (q) in such *Now* bias across delay times in intertemporal choice tasks (Smith et al. 2014; Takahashi 2009; Takahashi et al. 2008). Consistent with our ICR-based results, we found that lower FMT signal in the putamen predicted a significantly larger k_q value, relative to those with higher FMT signal in the putamen [$F_{(1,9)} = 10.59$, $P = 0.01$]. To reduce skew in the k_q distribution of values, we applied a $\log_{10}$ transformation to the k_q values prior to parametric analyses, with less negative $\log_{10}k_q$ values indicating more impulsive intertemporal choice at delay $D = 0$. We found significant differences between groups, indicating more impulsive choice at delay $D = 0$ in low putamen FMT individuals (Fig. 5*A*; Low putamen FMT $\log_{10}k_q$: −1.94 ± 0.71, High putamen FMT $\log_{10}k_q$: −3.39 ± 0.69). In contrast, we did not observe a

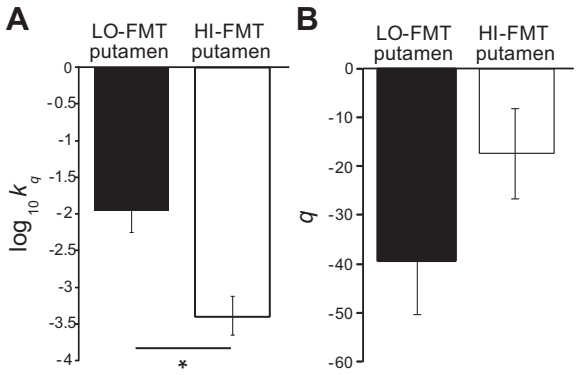

Fig. 5. Lower putamen FMT signal is specifically associated with more impulsive intertemporal choice, not greater inconsistency in intertemporal choices. *A*: covariate-adjusted $\log_{10}k_q$ (impulsivity) by putamen FMT group. Less negative $\log_{10}k_q$ values indicate more impulsive intertemporal choice at delay $D = 0$. $\text{Log}_{10}k_q$ values differed significantly between groups [$F_{(1,9)} = 10.59$, $^*P = 0.01$]. *B*: covariate-adjusted q (consistency). Less negative q values indicate more consistent intertemporal choice across delay times. The average q value did not differ significantly between groups [$F_{(1,9)} = 1.93$, $P = 0.198$]. Values reflect estimated marginal means ± SE. Conventions as for Fig. 3.

significant difference in q between Low and High putamen FMT groups [Fig. 5*B*; $F_{(1,9)} = 1.93$, $P = 0.198$]. Not surprisingly, given these findings, k_q was strongly correlated with ICR [Spearman's $\rho = 0.912$ (95% CI: 0.666, 0.983), $P < 0.001$], while the correlation between ICR and q was not significant [Spearman's $\rho = -0.220$ (95% CI: −0.752, 0.448), $P = 0.471$]. In addition, we quantified the time decay of the discount rate (k_q) across delay times using Prelec's (2004) measure of "decreasing impatience" (DI), which quantifies the degree to which k_q changes with increasing delay time, as implemented within the q-exponential discount function by Takahashi (2011). A rational (exponential) discount rate yields a DI of zero, while DI is positive for irrational intertemporal choice associated with preference reversal over increasing delay time. A repeated-measures ANOVA [putamen FMT (High/Low) × delay time] found significant main effects of both putamen FMT [$F_{(1,9)} = 8.71$, $P = 0.016$, $\eta^2 = 0.20$] and delay time [$F_{(4,36)} = 15.54$, $P < 0.001$, $\eta^2 = 0.41$] and a significant interaction between putamen FMT and delay time [$F_{(4,36)} = 7.35$, $P < 0.001$, $\eta^2 = 0.21$; Fig. 6]. Average DI_q across delay times was higher in the Low putamen FMT group (mean = 0.031; 95% CI: 0.017, 0.046) vs. the High putamen FMT group [mean = 0.013, 95% CI: 0.003, 0.027; $F_{(1,9)} = 8.71$, $P = 0.016$]. We confirmed the effect of delay time on DI_q with a Friedman's test on DI_q across delay times ($\chi^2 = 52$, $P < 0.001$, df = 4). Post hoc comparisons of DI_q between groups at each delay time showed significantly higher DI_q values associated with lower putamen FMT at all five delays [mean differences (bootstrapped): 7 days: 0.077, $F = 7.74$, $P = 0.021$; 14 days: 0.042, $F = 8.82$, $P = 0.016$; 30 days: 0.020, $F = 9.34$, $P = 0.014$; 90 days: 0.007, $F = 8.17$, $P = 0.019$; 180 days: 0.003, $F = 6.87$, $P = 0.028$]. These data indicate that lower FMT signal in the putamen predicts greater irrationality of intertemporal choice, with the greatest effects at the shortest delay and diminishing with increasing delay times.

Low midbrain FMT K_i predicts enhanced sensitivity of Now bias to increasing delayed reward amount. We also predicted greater *Now* bias (quantified as ICR) in those with relatively lower FMT K_i in the midbrain. However, in comparing the participants with midbrain FMT K_i values below the group median (Low midbrain FMT) to those above the group median (High midbrain FMT), we observed no significant difference in ICR in the Low midbrain FMT group (median = 0.534) relative to the High midbrain FMT group (median = 0.566) in a bootstrapped ANOVA [$F_{(1,11)} = 0.12$, $P = 0.738$, $\eta^2 = 0.009$; Fig. 7*A*]. We next evaluated ICR as a function of delay time (Fig. 7*B*). A mixed-effects 2 × 5 ANOVA found a significant main effect of delay time [$F_{(4,44)} = 5.65$; $P = 0.001$, $\eta^2 = 0.297$] but no significant effect of midbrain FMT group [$F_{(1,11)} = 0.21$; $P = 0.66$, $\eta^2 = 0.016$] or midbrain FMT × delay interaction [$F_{(4,44)} = 0.87$; $P = 0.49$, $\eta^2 = 0.045$]. We also evaluated *Now* bias (ICR) as a function of the delayed reward amount (Fig. 7*C*). A 2 × 5 mixed-effects ANOVA found a significant main effect of *Later* amount [$F_{(4,44)} = 5.01$; $P = 0.002$, $\eta^2 = 0.261$] but no significant main effect of midbrain FMT [$F_{(1,11)} = 0.19$; $P = 0.67$, $\eta^2 = 0.014$]. We did, however, observe a nearly statistically significant medium-size midbrain FMT × amount interaction [$F_{(4,44)} = 2.58$; $P = 0.050$, $\eta^2 = 0.134$]. Note that sex was included as a covariate in this analysis and did not have a significant effect ($P = 0.202$). Direct comparison of the slope and intercept terms of the logarithmic fit to each subject's ICR by *Later* amount data found significantly steeper slopes in the Low midbrain FMT group (mean = −0.32 ± 0.18) relative to the High midbrain FMT group [mean = −0.14 ± 0.10; $F_{(1,11)} = 5.75$, $P = 0.035$, $\eta^2 = 0.325$], while the intercepts showed no difference between midbrain FMT groups [Low midbrain FMT: mean = 0.93 ± 0.33; High midbrain FMT: mean = 0.66 ± 0.40; $F_{(1,11)} = 0.41$, $P = 0.54$, $\eta^2 = 0.034$]. These results indicate greater sensitivity to increasing reward magnitude in those with lower DA synthesis capacity in the midbrain.

As for the Low and High putamen FMT group comparisons, when comparing Low and High midbrain FMT groups we observed no group differences in objective choice (CON) trial accuracy [$F_{(1,11)} = 0.04$, $P = 0.85$], response consistency [$F_{(1,11)} = 0.001$, $P = 0.97$], or RT in the objective choice (CON) [$F_{(1,11)} = 0.05$, $P = 0.83$], or subjective choice [WANT: $F_{(1,11)} = 0.01$, $P = 0.92$; DON'T WANT: $F_{(1,11)} = 0.33$, $P = 0.58$] trials, indicating that differences in these measures of response control do not explain the enhanced

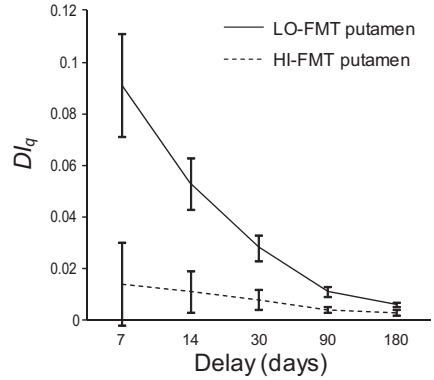

Fig. 6. Decreasing impatience (DI_q) as a function of delay time. DI_q is elevated in the Low putamen FMT group relative to the High putamen FMT group [$F_{(1,9)} = 8.71$, $P = 0.016$], and while DI_q declines as a function of delay in both groups, DI_q declines more steeply in the Low putamen FMT group, indicating more irrational intertemporal choice. Conventions as for Fig. 3.

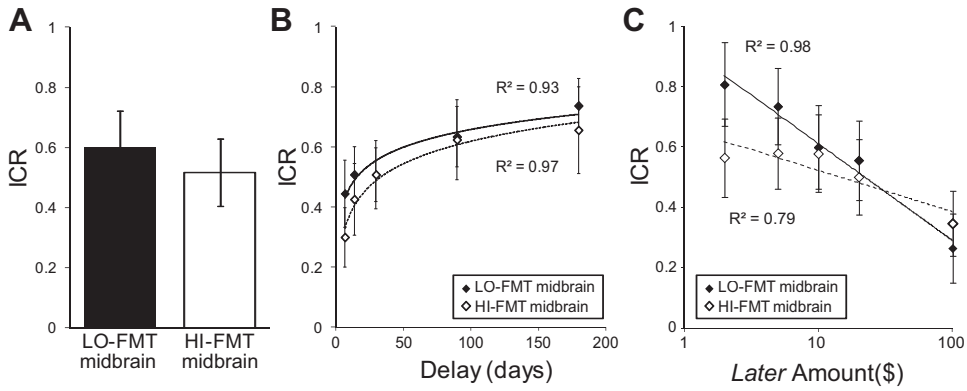

Fig. 7. Steeper reward magnitude discounting associated with Low midbrain FMT signal. *A*: *Now* bias does not differ in those with lower midbrain FMT. Plot depicts covariate-adjusted ICR in participants with below-median FMT signal in the midbrain (LO-FMT midbrain) and above-median FMT signal in the midbrain (HI-FMT midbrain). *B*: no significant differences are found for covariate-adjusted ICR as a function of delayed reward time in the Low midbrain FMT group vs. the High midbrain FMT group. *C*: semilog plots of covariate-adjusted ICR as a function of *Later* amount in the Low midbrain FMT group and the High midbrain FMT group. The average slope of the magnitude discounting curves was significantly greater in the Low midbrain FMT group [$F_{(1,11)} = 5.75$, $P = 0.035$]. Values reflect estimated marginal means ± SE. Lines represent logarithmic fit of the group averaged data, with regression terms shown for each group.

sensitivity of *Now*/*Later* choice to reward magnitude associated with Low midbrain FMT K_i.

Exploratory analyses of relationship between Now bias and FMT K_i in caudate and ventral striatum. In addition to the a priori analyses reported above, we conducted an exploratory investigation of the relationship between *Now* bias and FMT K_i in the caudate and in the ventral striatum. In contrast to our findings in the putamen, we found no significant association between *Now* bias and FMT K_i in either the bilateral ventral striatum ($\rho = -0.329$, $P = 0.213$; CI: −0.725, 0.163) or the bilateral caudate ($\rho = 0.182$, $P = 0.499$; CI: −0.419, 0.619). Furthermore, unlike our midbrain findings, we found no relationship between the slope of the ICR by delay reward amount (a measure of reward magnitude sensitivity) and FMT K_i in either the ventral striatum ($\rho = 0.279$, $P = 0.295$; CI: −0.256, 0.715) or the caudate ($\rho = 0$, $P = 1$; CI: −0.497, 0.458). No other measure of *Now* bias (area under the curve, criterion interest rate, or log *k*) was significantly associated with FMT K_i in the caudate or ventral striatum (min. $P = 0.362$).

General findings. Mean K_i values for the bilateral putamen and midbrain were 0.024 ± 0.001 and 0.009 ± 0.002, respectively. Mean K_i values for the bilateral caudate and ventral striatum were 0.019 ± 0.002 and 0.017 ± 0.002, respectively. As this study included both men and women over a range of ages (25–34 yr), it is important to consider whether either sex or age could have significantly contributed to our findings. We observed no significant differences between sexes in mean K_i in any of our areas of interest (min. $P = 0.261$). Moreover, we found no significant correlation between age and K_i in any of our areas of interest (min. $P = 0.582$). Thus sex and age are unlikely to be substantially impacting our findings. Finally, we note that in this small sample the trend toward *COMT* Val^{158}Met genotype to predict ICR did not reach statistical significance [$F_{(1,12)} = 2.627$, $P = 0.131$, $\eta^2 = 0.13$]; we did find a significant effect of *COMT* Val^{158}Met genotype on the closely related alternate measure of impulsive choice, k_q [$F_{(1,9)} = 5.531$, $P = 0.043$, $\eta^2 = 0.22$], consistent with our prior findings in adults (Boettiger et al. 2007; Smith and Boettiger 2012).

DISCUSSION

Here we demonstrate that relatively low DA synthesis capacity in the putamen of healthy young adults is associated with elevated *Now* bias, more irrational discounting at short delay times, and strikingly higher criterion interest rates. In contrast, we found that lower DA synthesis capacity in the midbrain predicted greater sensitivity to increasing reward magnitude. These effects were over and above those explained by putative frontal DA, based on *COMT* genotype. These data suggest that individual differences in subcortical DA synthesis independently contribute to variation in intertemporal choice when controlling for *COMT* genotype.

Impulsivity, dopamine, and the putamen. As noted in the introduction, some existing evidence links variations in the putamen specifically to individual differences in *Now* bias during intertemporal choice tasks. First, in adult men with ADHD with or without cocaine dependence, the degree to which methylphenidate increased DA signaling in the putamen predicted the drug's ability to decrease *Now* bias (Crunelle et al. 2013). Second, in a mixed population of control subjects and people with methamphetamine dependence, which included adults up to age 51 yr (the majority of whom were smokers), DA D_2/D_3 receptor binding in the whole striatum was inversely related to *Now* bias (Ballard et al. 2015). In examining striatal subdivisions, among the methamphetamine-dependent participants the putamen was the only subdivision that showed this relationship after accounting for effects of age. Age was in fact the strongest predictor of D_2/D_3 receptor binding, and effects of age and smoking may have occluded their ability to detect significant effects in the control subjects. Another recent PET paper examining temporal discounting in pathological gamblers and patients with Parkinson's disease also included a small sample of control subjects, again with a very large age range [coefficient of variation (CV) >3 times larger than the age CV for our study], finding no significant relationships among control subjects but significant correlations between ventral striatal DA and *Now* bias among gamblers and between putamen DA and *Now* bias among Parkinson's patients. Third, the degree to which tolcapone, a COMT inhibitor, increases activity in the putamen during *Now*/*Later*

choices significantly correlated with decreased *Now* bias on tolcapone in healthy adults (Kayser et al. 2012). In addition, fMRI data collected during intertemporal choice suggests that the dorsal striatum is involved in integrating subjective valuation systems sensitive to reward delay and magnitude, providing an overall value metric to guide choice behavior (Pine et al. 2009). Beyond these specific relationships between DA, the putamen, and *Now* bias, other work has linked DA signaling in the putamen to other measures of impulsivity. For example, in adult men, higher trait impulsivity as measured by the Barratt Impulsiveness Scale (BIS) scores negatively correlates with DAT availability in the dorsal striatum, particularly in the putamen (Costa et al. 2013). BIS scores also positively correlate with elevated amphetamine-induced striatal DA release in healthy adults (Buckholtz et al. 2010). In addition, in nonhuman primates impairments in inhibitory control are correlated with increased gray matter in the putamen (Groman et al. 2013) as well as with decreased DA signaling in the putamen (Groman et al. 2011, 2012, 2013). Moreover, fMRI studies have reported evidence of delay time sensitivity in the putamen during both intertemporal choice (Wittmann et al. 2007) and a monetary incentive delay (MID) task incorporating rewards available at different delays (Luo et al. 2009). All of these data are consistent with the present finding that reduced presynaptic DA availability in the putamen is associated with greater impulsivity. Future work linking PET markers of putamen DA, fMRI during intertemporal choice, and pharmacological effects on *Now* bias in the same subjects is needed to establish the mechanistic linkage between each of these lines of evidence.

A key point is that the putamen DA synthesis effects we observed were present after controlling for *COMT* genotype effects, suggesting that low cortical DA tone and low presynaptic DA availability in the putamen make independent contributions to immediate reward selection bias. This result could reflect differing contributions of frontal DA and putamen DA to intertemporal choice. For example, we have previously reported hyperactivation in dorsal prefrontal and posterior parietal cortex during intertemporal choice associated with the *COMT* Val/Val genotype (Boettiger et al. 2007), which is reminiscent of activity associated with inefficiency in working memory function (Tunbridge et al. 2006). This finding, coupled with evidence for numerical distance comparisons in the posterior parietal lobe (Pinel et al. 2001), suggests that *COMT* genotype may confer differences in the capacity to hold numerical calculations in mind that allow for efficient comparisons of relative magnitude during intertemporal reward choice. In contrast, perhaps DA availability in the putamen plays a greater role in time perception, another cognitive process thought to contribute to the discounting of delayed rewards (Takahashi 2011; Wittmann and Paulus 2008). Human lesion studies show that processing of numerosity and of time duration are independent (Cappelletti et al. 2011). Moreover, Parkinson's disease patients, who have deficits in DA signaling in the dorsal striatum, are selectively impaired in comparisons of duration but not of numerosity (Dormal et al. 2012). This latter finding is consistent with abundant evidence linking deficiencies in DA signaling with overestimation of time (see Merchant et al. 2013 for a recent review). While most work on timing has not explicitly distinguished between the caudate and the putamen, a recent pharmaco-fMRI study found that the effect of acute DA depletion on timing perception was specifically associated with a decrement in putamen activity when holding durations in mind (Coull et al. 2012). Alternatively, given evidence that the posterior putamen of primates is preferentially activated during automatic motor behaviors relative to nonroutine motor actions that require greater attention (Deffains et al. 2010), reduced FMT in the putamen could alternatively lead to greater impulsivity via reduced attention to action. Indeed, reduced DA signaling in the primate putamen is associated with impaired flexibility in response selection, which could reflect a common attention to action deficit (Groman et al. 2011).

Finally, prior PET studies with FMT or the related radioligand L-3,4-dihydroxy-6-[^{18}F]fluorophenylalanine (F-DOPA) interpret uptake of these tracers as an index of DA tone rather than phasic DA release (Braskie et al. 2011; Dreher et al. 2008; Kienast et al. 2008; Schlagenhauf et al. 2013; Siessmeier et al. 2006), a view further supported by combined F-DOPA and D_2/D_3 binding PET data from nonhuman primates (Doudet et al. 2004). According to this view, individuals with lower putamen FMT uptake in our study are more likely to release phasic DA bursts, which in turn favors more impulsive intertemporal choice.

Midbrain dopamine and impulsivity. In addition to the dorsal striatal findings described above, individual differences in trait impulsivity (as indexed by BIS scores) have also been associated with D_2/D_3 autoreceptor binding in the midbrain: diminished D_2/D_3 autoreceptor binding predicts greater impulsiveness (Buckholtz et al. 2010). Midbrain DA measures in humans have not previously been directly linked to DD, but data from animal models have shown that midbrain DA neurons are more active in response to higher-value rewards (Fiorillo et al. 2003; Roesch et al. 2007; Tobler et al. 2005), with Tobler and colleagues (2005) showing that the activity of midbrain DA neurons scales specifically with reward magnitude. In light of these data, our finding that relatively low midbrain DA synthesis capacity is associated with greater sensitivity to reward magnitude in an intertemporal reward choice task suggests two possible explanations. First, perhaps lower DA synthesis capacity in the midbrain neurons allows for a wider dynamic range of DA release in projection fields in response to rewards of different magnitudes. Alternatively, perhaps lower midbrain DA synthesis capacity reduces autoinhibition of midbrain DA neurons via somatodendritic DA release (Adell and Artigas 2004), which could also theoretically expand the dynamic range of DA neuron firing to differing reward magnitudes. Future studies using pharmacogenetic tools to precisely manipulate local vs. distal DA release will be needed to shed light on this issue. Alternatively, advances in dynamic pharmaco-PET imaging may allow disambiguation of these alternatives.

What about the ventral striatum/nucleus accumbens? Some fMRI studies of intertemporal choice have implicated the ventral striatum/nucleus accumbens (nAc) in impulsive choice (e.g., McClure et al. 2004), with some studies specifically linking nAc activation to delayed reward magnitude sensitivity (Ballard and Knutson 2009). Moreover, fMRI measures of sensitivity to reward and punishment in the ventral striatum positively correlate with separately evaluated *Now* bias (Hariri et al. 2006). As such, we might have expected to find that differences in DA synthesis capacity in the nAc accounted for some of the individual differences in either *Now* bias or reward

magnitude sensitivity in the present data set. A possible explanation may be that the lumping of nAc core and shell regions, due to the low spatial resolution of PET, resulted in a canceling out of effects. This idea is supported from evidence in rodents that DA in the core and shell regions of the nAc have distinct functions. Specifically, DA D_2 receptor blockade in the core and shell have opposing effects on impulsivity, with increasing impulsivity consequent to core blockade and decreasing impulsivity with shell blockade (Besson et al. 2010). Likewise, DA release in the nAc shell scales with reward magnitude (Beyene et al. 2010), and inactivating the nAc shell decreases preference for larger vs. smaller rewards (Stopper and Floresco 2011). Furthermore, a reward-predicting cue elicits increases in phasic DA release in both the nAc core and shell, but such DA increases are greater and more sustained in the shell (Cacciapaglia et al. 2012). Recent fMRI work in humans further supports the distinctions between reward encoding in the nAc core and shell (Baliki et al. 2013) and suggests that future high-resolution PET imaging that allows disambiguation of DA signaling in these regions in humans may prove informative.

Conclusions. We acknowledge some limitations of the present study. First, our sample size is rather modest, so although some effect sizes were rather large, these findings bear replicating. Second, we did not test female participants within a fixed window of the menstrual cycle, which could impact *Now* bias (Smith et al. 2014). However, this concern is somewhat mitigated by the fact that the FMT-PET measures used in these analyses may be downstream of the hormonal effects (Kritzer and Kohama 1998, 1999; Pasqualini et al. 1995; Shansky et al. 2004; Xiao and Becker 1994) and thus predict *Now*/*Later* choice behavior independent of cycle phase. Regardless, these data add significantly to our existing model that frontal DA modulates *Now* bias according to a U-shaped function (Altamirano et al. 2011; Kelm and Boettiger 2013; Smith and Boettiger 2012; Smith et al. 2014) by identifying roles for specific extrastriatal DA terminal fields in modulating *Now* bias. Specifically, elevated *Now* bias was associated with lower putamen FMT signal, independent of *COMT* genotype. In contrast, lower midbrain FMT signal predicted greater sensitivity to increasing *Later* reward magnitude. This is the strongest demonstration that intertemporal reward choice in healthy young adult humans varies with region-specific measures of DA processing, with distinct regional associations with sensitivity to delay time and to reward magnitude. These findings support the hypothesis that the elevated *Now* bias in human alcoholics above that attributed to *COMT* genotype (Boettiger et al. 2007) may be accounted for by decreased DA synthesis capacity in the putamen. Future studies combining FMT-PET with measures of *Now* bias comparing alcoholics with control subjects are needed to test this idea.

ACKNOWLEDGMENTS

The authors thank H. S. Oppler, J. Cote, and T. Stokes for technical assistance.

GRANTS

This work was supported by National Institutes of Health (NIH) Grants UL1 RR-025747, KL2 RR-025746, P60 AA-011605, and the Foundation for Alcohol Research/ABMRF (C. A. Boettiger), by NIH Grants T32 DA-007244 and F31 AA-020132 (C. T. Smith), R01 DA-20600 (M. D'Esposito), F32 DA-027684 (D. L. Wallace), and AG-044292 (W. J. Jagust), and by the Niels Stensen Foundation (E. Aarts).

DISCLOSURES

No conflicts of interest, financial or otherwise, are declared by the author(s).

AUTHOR CONTRIBUTIONS

Author contributions: C.T.S., D.L.W., L.C.D., and C.A.B. analyzed data; C.T.S., W.J.J., M.D., and C.A.B. interpreted results of experiments; C.T.S., L.C.D., and C.A.B. prepared figures; C.T.S., D.L.W., L.C.D., E.A., M.D., and C.A.B. edited and revised manuscript; C.T.S., D.L.W., L.C.D., E.A., W.J.J., M.D., and C.A.B. approved final version of manuscript; D.L.W., W.J.J., and C.A.B. conception and design of research; D.L.W., L.C.D., E.A., and W.J.J. performed experiments; C.A.B. drafted manuscript.

REFERENCES

Acheson A, de Wit H. Bupropion improves attention but does not affect impulsive behavior in healthy young adults. *Exp Clin Psychopharmacol* 16: 113–123, 2008.

Adell A, Artigas F. The somatodendritic release of dopamine in the ventral tegmental area and its regulation by afferent transmitter systems. *Neurosci Biobehav Rev* 28: 415–431, 2004.

Alessi SM, Petry NM. Pathological gambling severity is associated with impulsivity in a delay discounting procedure. *Behav Processes* 64: 345–354, 2003.

Altamirano LJ, Fields HL, D'Esposito M, Boettiger CA. Interaction between family history of alcoholism and locus of control in the opioid regulation of impulsive responding under the influence of alcohol. *Alcohol Clin Exp Res* 35: 1905–1914, 2011.

Anokhin AP, Golosheykin S, Grant JD, Heath AC. Heritability of delay discounting in adolescence: a longitudinal twin study. *Behav Genet* 41: 175–183, 2011.

Ashburner J, Barnes G, Chen C, Daunizeau J, Flandin G, Friston K, Gitelman D, Kiebel S, Kilner J, Litvak V. *SPM8 Manual*. London: Functional Imaging Laboratory, Institute of Neurology, 2008.

Baliki MN, Mansour A, Baria AT, Huang L, Berger SE, Fields HL, Apkarian AV. Parceling human accumbens into putative core and shell dissociates encoding of values for reward and pain. *J Neurosci* 33: 16383–16393, 2013.

Ballard K, Knutson B. Dissociable neural representations of future reward magnitude and delay during temporal discounting. *Neuroimage* 45: 143–150, 2009.

Ballard ME, Mandelkern MA, Monterosso JR, Hsu E, Robertson CL, Ishibashi K, Dean AC, London ED. Low dopamine D2/D3 receptor availability is associated with steep discounting of delayed rewards in methamphetamine dependence. *Int J Neuropsychopharmacol* 18: pyu119, 2015.

Barkley RA, Edwards G, Laneri M, Fletcher K, Metevia L. Executive functioning, temporal discounting, and sense of time in adolescents with attention deficit hyperactivity disorder (ADHD) and oppositional defiant disorder (ODD). *J Abnorm Child Psychol* 29: 541–556, 2001.

Becker GS, Murphy KM. A theory of rational addiction. *J Political Econ* 96: 675–700, 1988.

Besson M, Belin D, McNamara R, Theobald DE, Castel A, Beckett VL, Crittenden BM, Newman AH, Everitt BJ, Robbins TW, Dalley JW. Dissociable control of impulsivity in rats by dopamine d2/3 receptors in the core and shell subregions of the nucleus accumbens. *Neuropsychopharmacology* 35: 560–569, 2010.

Beyene M, Carelli RM, Wightman RM. Cue-evoked dopamine release in the nucleus accumbens shell tracks reinforcer magnitude during intracranial self-stimulation. *Neuroscience* 169: 1682–1688, 2010.

Boettiger CA, Mitchell JM, Tavares VC, Robertson M, Joslyn G, D'Esposito M, Fields HL. Immediate reward bias in humans: frontoparietal networks and a role for the catechol-*O*-methyltransferase $158^{Val/Val}$ genotype. *J Neurosci* 27: 14383–14391, 2007.

Braskie MN, Landau SM, Wilcox CE, Taylor SD, O'Neil JP, Baker SL, Madison CM, Jagust WJ. Correlations of striatal dopamine synthesis with default network deactivations during working memory in younger adults. *Hum Brain Mapp* 32: 947–961, 2011.

Braskie MN, Wilcox CE, Landau SM, O'Neil JP, Baker SL, Madison CM, Kluth JT, Jagust WJ. Relationship of striatal dopamine synthesis capacity to age and cognition. *J Neurosci* 28: 14320–14328, 2008.

Buckholtz JW, Treadway MT, Cowan RL, Woodward ND, Li R, Ansari MS, Baldwin RM, Schwartzman AN, Shelby ES, Smith CE, Kessler RM, Zald DH. Dopaminergic network differences in human impulsivity. *Science* 329: 532, 2010.

Cacciapaglia F, Saddoris MP, Wightman RM, Carelli RM. Differential dopamine release dynamics in the nucleus accumbens core and shell track distinct aspects of goal-directed behavior for sucrose. *Neuropharmacology* 62: 2050–2056, 2012.

Cappelletti M, Freeman ED, Cipolotti L. Numbers and time doubly dissociate. *Neuropsychologia* 49: 3078–3092, 2011.

Cools R, Frank MJ, Gibbs SE, Miyakawa A, Jagust W, D'Esposito M. Striatal dopamine predicts outcome-specific reversal learning and its sensitivity to dopaminergic drug administration. *J Neurosci* 29: 1538–1543, 2009.

Costa A, la Fougère C, Pogarell O, Möller HJ, Riedel M, Ettinger U. Impulsivity is related to striatal dopamine transporter availability in healthy males. *Psychiatry Res* 211: 251–256, 2013.

Coull JT, Hwang HJ, Leyton M, Dagher A. Dopamine precursor depletion impairs timing in healthy volunteers by attenuating activity in putamen and supplementary motor area. *J Neurosci* 32: 16704–16715, 2012.

Crunelle CL, van den Brink W, Veltman DJ, van Emmerik-van Oortmerssen K, Dom G, Schoevers RA, Booij J. Low dopamine transporter occupancy by methylphenidate as a possible reason for reduced treatment effectiveness in ADHD patients with cocaine dependence. *Eur Neuropsychopharmacol* 23: 1714–1723, 2013.

Dalley JW, Mar AC, Economidou D, Robbins TW. Neurobehavioral mechanisms of impulsivity: fronto-striatal systems and functional neurochemistry. *Pharmacol Biochem Behav* 90: 250–260, 2008.

de Wit H. Impulsivity as a determinant and consequence of drug use: a review of underlying processes. *Addict Biol* 14: 22–31, 2009.

de Wit H, Enggasser JL, Richards JB. Acute administration of D-amphetamine decreases impulsivity in healthy volunteers. *Neuropsychopharmacology* 27: 813–825, 2002.

Deffains M, Legallet E, Apicella P. Modulation of neuronal activity in the monkey putamen associated with changes in the habitual order of sequential movements. *J Neurophysiol* 104: 1355–1369, 2010.

DeJesus OT. Positron labeled DOPA analogs to image dopamine terminals. *Drug Dev Res* 59: 249–260, 2003.

Dormal V, Grade S, Mormont E, Pesenti M. Dissociation between numerosity and duration processing in aging and early Parkinson's disease. *Neuropsychologia* 50: 2365–2370, 2012.

Doudet D, Cornfeldt M, Honey C, Schweikert A, Allen R. PET imaging of implanted human retinal pigment epithelial cells in the MPTP-induced primate model of Parkinson's disease. *Exp Neurol* 189: 361–368, 2004.

Doya K. Modulators of decision making. *Nat Neurosci* 11: 410–416, 2008.

Dreher JC, Meyer-Lindenberg A, Kohn P, Berman KF. Age-related changes in midbrain dopaminergic regulation of the human reward system. *Proc Natl Acad Sci USA* 105: 15106–15111, 2008.

Eisenberg D, MacKillop J, Modi M, Beauchemin J, Dang D, Lisman S, Lum JK, Wilson D. Examining impulsivity as an endophenotype using a behavioral approach: a DRD2 TaqI A and DRD4 48-bp VNTR association study. *Behav Brain Funct* 3: 2, 2007.

Fiorillo CD, Tobler PN, Schultz W. Discrete coding of reward probability and uncertainty by dopamine neurons. *Science* 299: 1898–1902, 2003.

Gogos JA, Morgan M, Luine V, Santha M, Ogawa S, Pfaff D, Karayiorgou M. Catechol-*O*-methyltransferase-deficient mice exhibit sexually dimorphic changes in catecholamine levels and behavior. *Proc Natl Acad Sci USA* 95: 9991–9996, 1998.

Groman S, Morales A, Lee B, London E, Jentsch J. Methamphetamine-induced increases in putamen gray matter associate with inhibitory control. *Psychopharmacology* 229: 527–538, 2013.

Groman SM, Lee B, London ED, Mandelkern MA, James AS, Feiler K, Rivera R, Dahlbom M, Sossi V, Vandervoort E, Jentsch JD. Dorsal striatal D2-like receptor availability covaries with sensitivity to positive reinforcement during discrimination learning. *J Neurosci* 31: 7291–7299, 2011.

Groman SM, Lee B, Seu E, James AS, Feiler K, Mandelkern MA, London ED, Jentsch JD. Dysregulation of D2-mediated dopamine transmission in monkeys after chronic escalating methamphetamine exposure. *J Neurosci* 32: 5843–5852, 2012.

Hamidovic A, Kang UJ, de Wit H. Effects of low to moderate acute doses of pramipexole on impulsivity and cognition in healthy volunteers. *J Clin Psychopharmacol* 28: 45–51, 2008.

Hariri AR, Brown SM, Williamson DE, Flory JD, de Wit H, Manuck SB. Preference for immediate over delayed rewards is associated with magnitude of ventral striatal activity. *J Neurosci* 26: 13213–13217, 2006.

Housden CR, O'Sullivan SS, Joyce EM, Lees AJ, Roiser JP. Intact reward learning but elevated delay discounting in Parkinson's disease patients with impulsive-compulsive spectrum behaviors. *Neuropsychopharmacology* 35: 2155–2164, 2010.

Jordan S, Eberling JL, Bankiewicz KS, Rosenberg D, Coxson PG, Van-Brocklin HF, O'Neil JP, Emborg ME, Jagust WJ. 6-[^{18}F]fluoro-L-*m*-tyrosine: metabolism, positron emission tomography kinetics, and 1-methyl-4-phenyl-1,2,3,6-tetrahydropyridine lesions in primates. *Brain Res* 750: 264–276, 1997.

Joutsa J, Voon V, Johansson J, Niemelä S, Bergman J, Kaasinen V. Dopaminergic function and intertemporal choice. *Transl Psychiatry* 5: e491, 2015.

Kaenmaki M, Tammimaki A, Myohanen T, Pakarinen K, Amberg C, Karayiorgou M, Gogos JA, Mannisto PT. Quantitative role of COMT in dopamine clearance in the prefrontal cortex of freely moving mice. *J Neurochem* 114: 1745–1755, 2010.

Karoum F, Chrapusta SJ, Egan MF. 3-Methoxytyramine is the major metabolite of released dopamine in the rat frontal cortex: reassessment of the effects of antipsychotics on the dynamics of dopamine release and metabolism in the frontal cortex, nucleus accumbens, and striatum by a simple two pool model. *J Neurochem* 63: 972–979, 1994.

Kayser AS, Allen DC, Navarro-Cebrian A, Mitchell JM, Fields HL. Dopamine, corticostriatal connectivity, and intertemporal choice. *J Neurosci* 32: 9402–9409, 2012.

Kelm MK, Boettiger CA. Effects of acute dopamine precusor depletion on immediate reward selection bias and working memory depend on catechol-*O*-methyltransferase genotype. *J Cogn Neurosci* 25: 2061–2071, 2013.

Kienast T, Siessmeier T, Wrase J, Braus DF, Smolka MN, Buchholz HG, Rapp M, Schreckenberger M, Rösch F, Cumming P. Ratio of dopamine synthesis capacity to D2 receptor availability in ventral striatum correlates with central processing of affective stimuli. *Eur J Nucl Med Mol Imaging* 35: 1147–1158, 2008.

Kritzer MF, Kohama SG. Ovarian hormones influence the morphology, distribution, and density of tyrosine hydroxylase immunoreactive axons in the dorsolateral prefrontal cortex of adult rhesus monkeys. *J Comp Neurol* 395: 1–17, 1998.

Kritzer MF, Kohama SG. Ovarian hormones differentially influence immunoreactivity for dopamine beta-hydroxylase, choline acetyltransferase, and serotonin in the dorsolateral prefrontal cortex of adult rhesus monkeys. *J Comp Neurol* 409: 438–451, 1999.

Lachman HM, Papolos DF, Saito T, Yu YM, Szumlanski CL, Weinshilboum RM. Human catechol-*O*-methyltransferase pharmacogenetics: description of a functional polymorphism and its potential application to neuropsychiatric disorders. *Pharmacogenetics* 6: 243–250, 1996.

Landau SM, Lal R, O'Neil JP, Baker S, Jagust WJ. Striatal dopamine and working memory. *Cereb Cortex* 19: 445–454, 2009.

Leeman RF, Potenza MN. Similarities and differences between pathological gambling and substance use disorders: a focus on impulsivity and compulsivity. *Psychopharmacology* 219: 469–490, 2012.

Logan J. Graphical analysis of PET data applied to reversible and irreversible tracers. *Nucl Med Biol* 27: 661–670, 2000.

Luo S, Ainslie G, Giragosian L, Monterosso JR. Behavioral and neural evidence of incentive bias for immediate rewards relative to preference-matched delayed rewards. *J Neurosci* 29: 14820–14827, 2009.

Mai JK, Assheuer J, Paxinos G. *Atlas of the Human Brain*. San Diego, CA: Academic, 1997.

Mawlawi O, Martinez D, Slifstein M, Broft A, Chatterjee R, Hwang DR, Huang Y, Simpson N, Ngo K, Van Heertum R, Laruelle M. Imaging human mesolimbic dopamine transmission with positron emission tomography. I. Accuracy and precision of D_2 receptor parameter measurements in ventral striatum. *J Cereb Blood Flow Metab* 21: 1034–1057, 2001.

Mazur JE. An adjusting procedure for studying delayed reinforcement. In: *Quantitative Analyses of Behavior*. Hillsdale, NJ: Erlbaum, 1987.

McClure SM, Laibson DI, Loewenstein G, Cohen JD. Separate neural systems value immediate and delayed monetary rewards. *Science* 306: 503–507, 2004.

Merchant H, Harrington DL, Meck WH. Neural basis of the perception and estimation of time. *Annu Rev Neurosci* 36: 313–336, 2013.

Milenkova M, Mohammadi B, Kollewe K, Schrader C, Fellbrich A, Wittfoth M, Dengler R, Münte TF. Intertemporal choice in Parkinson's disease. *Mov Disord* 26: 2004–2010, 2011.

Mitchell JM, Fields HL, D'Esposito M, Boettiger CA. Impulsive responding in alcoholics. *Alcohol Clin Exp Res* 29: 2158–2169, 2005.

Mitchell JM, Tavares VC, Fields HL, D'Esposito M, Boettiger CA. Endogenous opioid blockade and impulsive responding in alcoholics and healthy controls. *Neuropsychopharmacology* 32: 439–449, 2007.

Mitchell SH. The genetic basis of delay discounting and its genetic relationship to alcohol dependence. *Behav Processes* 87: 10–17, 2011.

Paloyelis Y, Asherson P, Mehta MA, Faraone SV, Kuntsi J. DAT1 and COMT effects on delay discounting and trait impulsivity in male adolescents with attention deficit/hyperactivity disorder and healthy controls. *Neuropsychopharmacology* 35: 2414–2426, 2010.

Pasqualini C, Olivier V, Guibert B, Frain O, Leviel V. Acute stimulatory effect of estradiol on striatal dopamine synthesis. *J Neurochem* 65: 1651–1657, 1995.

Patlak CS, Blasberg RG. Graphical evaluation of blood-to-brain transfer constants from multiple-time uptake data. Generalizations. *J Cereb Blood Flow Metab* 5: 584–590, 1985.

Pine A, Seymour B, Roiser JP, Bossaerts P, Friston KJ, Curran HV, Dolan RJ. Encoding of marginal utility across time in the human brain. *J Neurosci* 29: 9575–9581, 2009.

Pine A, Shiner T, Seymour B, Dolan RJ. Dopamine, time, and impulsivity in humans. *J Neurosci* 30: 8888–8896, 2010.

Pinel P, Dehaene S, Riviere D, LeBihan D. Modulation of parietal activation by semantic distance in a number comparison task. *Neuroimage* 14: 1013–1026, 2001.

Prelec D. Decreasing impatience: a criterion for non-stationary time preference and "hyperbolic" discounting. *Scand J Econ* 106: 511–532, 2004.

Rachlin H. *The Science of Self-Control*. Cambridge, MA: Harvard Univ. Press, 2000, p. 220.

Reynolds B. A review of delay-discounting research with humans: relations to drug use and gambling. *Behav Pharmacol* 17: 651–667, 2006.

Roesch MR, Calu DJ, Schoenbaum G. Dopamine neurons encode the better option in rats deciding between differently delayed or sized rewards. *Nat Neurosci* 10: 1615–1624, 2007.

Schlagenhauf F, Rapp MA, Huys QJ, Beck A, Wüstenberg T, Deserno L, Buchholz HG, Kalbitzer J, Buchert R, Bauer M. Ventral striatal prediction error signaling is associated with dopamine synthesis capacity and fluid intelligence. *Hum Brain Mapp* 34: 1490–1499, 2013.

Shansky RM, Glavis-Bloom C, Lerman D, McRae P, Benson C, Miller K, Cosand L, Horvath TL, Arnsten AF. Estrogen mediates sex differences in stress-induced prefrontal cortex dysfunction. *Mol Psychiatry* 9: 531–538, 2004.

Siessmeier T, Kienast T, Wrase J, Larsen JL, Braus DF, Smolka MN, Buchholz HG, Schreckenberger M, Rösch F, Cumming P. Net influx of plasma 6-[^{18}F]fluoro-L-DOPA (FDOPA) to the ventral striatum correlates with prefrontal processing of affective stimuli. *Eur J Neurosci* 24: 305–313, 2006.

Slifstein M, Kolachana B, Simpson EH, Tabares P, Cheng B, Duvall M, Frankle WG, Weinberger DR, Laruelle M, Abi-Dargham A. COMT genotype predicts cortical-limbic D1 receptor availability measured with [^{11}C]NNC112 and PET. *Mol Psychiatry* 13: 821–827, 2008.

Smith CT, Boettiger CA. Age modulates the effect of COMT genotype on delay discounting behavior. *Psychopharmacology* 222: 609–617, 2012.

Smith CT, Sierra Y, Oppler SH, Boettiger CA. Ovarian cycle effects on immediate reward selection bias in humans: a role for estradiol. *J Neurosci* 34: 5468–5476, 2014.

Sonuga-Barke EJ, Sergeant JA, Nigg J, Willcutt E. Executive dysfunction and delay aversion in attention deficit hyperactivity disorder: nosologic and diagnostic implications. *Child Adolesc Psychiatric Clin N Am* 17: 367–384, ix, 2008.

Stopper CM, Floresco SB. Contributions of the nucleus accumbens and its subregions to different aspects of risk-based decision making. *Cogn Affect Behav Neurosci* 11: 97–112, 2011.

Takahashi T. Theoretical frameworks for neuroeconomics of intertemporal choice. *J Neurosci Psychol Econ* 2: 75, 2009.

Takahashi T. A neuroeconomic theory of rational addiction and nonlinear time-perception. *Neuroendocrinol Lett* 32: 221–225, 2011.

Takahashi T, Oono H, Radford MH. Psychophysics of time perception and intertemporal choice models. *Physica A Stat Mech Applications* 387: 2066–2074, 2008.

Tobler PN, Fiorillo CD, Schultz W. Adaptive coding of reward value by dopamine neurons. *Science* 307: 1642–1645, 2005.

Tunbridge EM, Harrison PJ, Weinberger DR. Catechol-*O*-methyltransferase, cognition, and psychosis: Val158Met and beyond. *Biol Psychiatry* 60: 141–151, 2006.

VanBrocklin HF, Blagoev M, Hoepping A, O'Neil JP, Klose M, Schubiger PA, Ametamey S. A new precursor for the preparation of 6-[^{18}F]fluoro-L-*m*-tyrosine ([^{18}F]FMT): efficient synthesis and comparison of radiolabeling. *Appl Radiat Isot* 61: 1289–1294, 2004.

Vingerhoets FJ, Snow BJ, Tetrud JW, Langston JW, Schulzer M, Calne DB. Positron emission tomographic evidence for progression of human MPTP-induced dopaminergic lesions. *Ann Neurol* 36: 765–770, 1994.

Winstanley CA. The utility of rat models of impulsivity in developing pharmacotherapies for impulse control disorders. *Br J Pharmacol* 164: 1301–1321, 2011.

Wittmann M, Leland D, Paulus M. Time and decision making: differential contribution of the posterior insular cortex and the striatum during a delay discounting task. *Exp Brain Res* 179: 643–653, 2007.

Wittmann M, Paulus MP. Decision making, impulsivity and time perception. *Trends Cogn Sci* 12: 7–12, 2008.

Wu K, O'Keeffe D, Politis M, O'Keeffe GC, Robbins TW, Bose SK, Brooks DJ, Piccini P, Barker RA. The catechol-*O*-methyltransferase Val^{158}Met polymorphism modulates fronto-cortical dopamine turnover in early Parkinson's disease: a PET study. *Brain* 135: 2449–2457, 2012.

Xiao L, Becker JB. Quantitative microdialysis determination of extracellular striatal dopamine concentration in male and female rats: effects of estrous cycle and gonadectomy. *Neurosci Lett* 180: 155–158, 1994.